Electron Correlations, Magnetism, and Structure of Small Clusters

G. M. Pastor, R. Hirsch, and B. Mühlschlegel
Institut für Theoretische Physik der Universität zu Köln, Zülpicher Strasse 77, 50937 Köln, Germany
(Received 15 December 1993)

Many-body properties of N-atom clusters having $N \leq 8$ are calculated exactly in the framework of the Hubbard model for all possible nonequivalent cluster structures. The most stable structure and the corresponding total spin S are obtained rigorously as a function of the Coulomb-interaction strength U/t and the number of electrons. Results for the stability of cluster ferromagnetism against electronic excitations and structural changes are obtained for the first time. The resulting interplay between electron correlations, magnetism, and cluster structure is determined.

PACS numbers: 75.10.Lp, 36.40.+d, 75.60.Jp

Magnetism is one of the most interesting and challenging problems in cluster physics. The major part of the experimental and theoretical work in this field has been dedicated to the study of $3d$ transition metals (TM) due to their central importance in both basic and applied science [1–4]. From a fundamental point of view, these clusters offer a unique opportunity to study how the magnetic properties change as the localized electrons of an isolated atom start to delocalize throughout several atoms, and how the itinerant magnetism characteristic of the solid state develops with increasing cluster size. Moreover, the magnetic behavior of itinerant $3d$ electrons is known to be very sensitive to the lattice structure and to the local environment of the atoms [3–7]. The determination of the relation between cluster structure and magnetism, and of the stability of cluster ferromagnetism against structural changes as well as electronic excitations, is therefore crucial for the progress in this field.

The theoretical understanding of cluster magnetism is hindered by two main difficulties: an accurate treatment of *electron correlations,* which are fundamental for magnetism, and a thorough optimization of the *cluster geometry,* on which the magnetic properties of itinerant electrons are known to depend strongly. Since these two problems are formidable and their combination even more so, it is natural that the studies performed so far have attempted to deal with one of them at a time [3–8]. It is the goal of this Letter to present the first complete many-body study of magnetism and cluster structure, where these two important aspects are treated rigorously and on the same electronic level.

In order to achieve rigorous theoretical results on such a complex problem, one is forced to consider a model which is simple enough to allow an exact or at least very accurate solution, and which at the same time contains enough complexity to be able to shed light on the physics of real systems (e.g., $3d$ TM). Such a model is given by the Hubbard Hamiltonian [9]:

$$H = -t \sum_{\langle i,j\rangle,\sigma} c^{\dagger}_{i\sigma} c_{j\sigma} + U \sum_{i} n_{i\uparrow} n_{i\downarrow} . \qquad (1)$$

In spite of its simplicity, this Hamiltonian has played, together with related models, a major role in guiding our understanding of the many-body properties of metals and particularly of magnetism in both three- and low-dimensional systems. It is our aim to use it now to determine the magnetic and structural properties of small clusters and their interplay. The underlying electron correlation problem is solved *exactly* within a full many-body scheme, and a complete geometry optimization is performed by considering *all possible* nonequivalent cluster structures. In this way, definitive conclusions about the behavior of clusters within the Hubbard model are achieved for the first time.

In order to solve the problem of geometry optimization completely, it should first be noted that in the Hubbard model only the topological aspect of the structure is relevant for the electronic properties or, in other words, defining the cluster structure is equivalent to defining for each atom i those atoms j which are connected to i by the hopping element t. The set of all possible nonequivalent cluster structures is, therefore, a subset of the set of graphs with N vertices [8]. We generate all possible graphs by considering the adjacency matrix A which characterizes a graph: $A_{ij} = 1$ if i and j are nearest neighbors (NN), and $A_{ij} = 0$ otherwise. A set of nonequivalent A's is obtained by means of a simple bit-operation computer algorithm [10]. However, notice that for the study of clusters, we must consider only those graphs which can be represented as a three-dimensional structure. For that reason, a *graph* is accepted as a possible cluster *structure,* if a set of atomic coordinates exists, such that the interatomic distances R_{ij} satisfy the conditions $R_{ij} = R_0$ if $A_{ij} = 1$ (i.e., NN), and $R_{ij} > R_0$ otherwise, where R_0 refers to the NN distance [11].

The optimal cluster structure is determined as a function of U/t and of the number of electrons ν by comparing the ground-state energies of all possible nonequivalent structures [12]. These energies are calculated by means of Lanczos' iterative method [13]. In this full many-body scheme, the correlated ground-state energy E is obtained *exactly* within a controlled accuracy ε (in our case $\varepsilon \simeq 10^{-10}$) [14]. The convergence of E is monitored as a function of the number of iterations M and the sequence

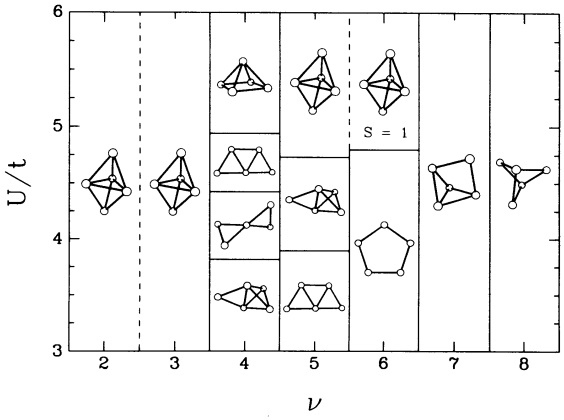

FIG. 1. Phase diagram of Hubbard clusters having $N = 5$ atomic sites. The ground-state structures obtained for a Coulomb repulsion U, hopping integral t, and number of electrons ν are illustrated. The ground-state spin S is minimal (i.e., $S = 0$ or $S = 1/2$) unless indicated. For $\nu = 4$, $S = 1$ for $U/t > 29.9$, and for $\nu = 6$, $S = 2$ for $U/t > 10.8$. No further structural changes are found for $0 \leq U/t \leq 3$ and $U/t \geq 6$.

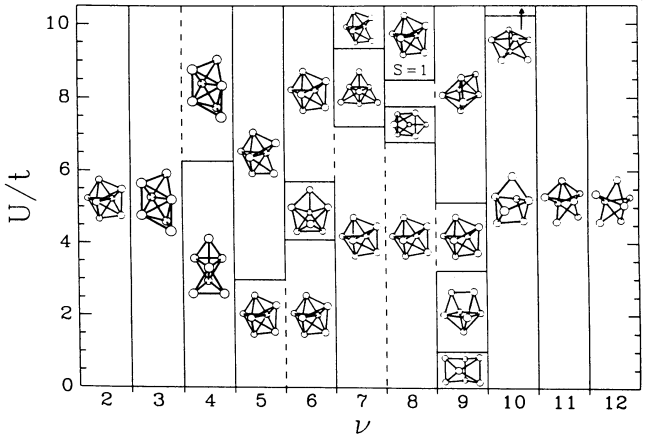

FIG. 2. Phase diagram of Hubbard clusters having $N = 7$ sites as in Fig. 1. Results for $U/t > 10$ are given in Fig. 3.

is interrupted once $|E(M) - E(M - m)|/|E(M)| < \varepsilon$ ($m \simeq 5$). Comparison with previous work [5–8] and with direct numerical diagonalizations shows that ε is not underestimated. The error ε is taken into account when comparing the energies of the different cluster structures (e.g., two structures are considered to be degenerate if their energy difference is less than the sum of the estimated errors). Therefore, our results for the most stable geometries are rigorous, although strictly speaking the energies cannot be calculated exactly. Once the ground-state structure has been identified, we calculate the ground-state eigenvector from which the observables like the total spin S are accurately derived. Using an appropriate projector several excited-state energies for different S are also obtained, which give direct information about the stability of magnetism.

The results for the most stable structure and total spin S as a function of the Coulomb interaction strength U/t and number of electrons ν are summarized in the form of "phase" or structural diagrams as the ones shown in Figs. 1–3 [15]. The main conclusions and trends derived from our calculations for $N \leq 8$ are discussed below [10].

For low electron or hole concentration (i.e., $\nu/N \leq 0.4$–0.6 and $2 - \nu/N \leq 0.3$–0.6) the optimal cluster structure is independent of U/t, i.e., the structure which yields the minimal kinetic energy (uncorrelated limit) remains the most stable one, irrespective of the strength of the Coulomb interactions. Furthermore, no magnetic transitions are observed: the ground state is always a singlet or a doublet (see Figs. 1–3). This indicates that, for low carrier concentration, the Coulomb interactions are very efficiently suppressed by the correlations, so that the magnetic and geometric structure of the clusters are dominated by the kinetic term. This physically plausible conclusion is further supported by analytical results for the case of two carriers [10]. Nonetheless, the fact that this holds for finite values of ν/N and $U/t \to +\infty$ seems not obvious *a priori*.

For small ν we obtain compact structures having maximal average coordination number $\bar{z}$ ($t > 0$). These are all substructures of the icosahedron and have the largest possible number of *triangular* loops. In contrast, for large ν (small $\nu_h = 2N - \nu$) open ground-state structures are found. In particular for $\nu_h = 2$ we obtain bipartite structures, which have the largest possible number of *square* loops. This can be qualitatively understood in terms of the single-particle spectrum. In the first case (small ν) the largest stability is obtained for the largest bandwidth for bonding (negative-energy) states ($\varepsilon_b \leq -\bar{z}t$), while in the second case (small ν_h) it is obtained for the largest bandwidth for antibonding (positive-energy) states, i.e., for the most compact bipartite structure.

A much more interesting interplay between electronic correlations, magnetism, and cluster structure is observed around half-band filling (i.e., $|\nu/N - 1| \leq 0.2$–0.4). Here, several structural transitions are found as a function of U/t (see Figs. 1–3). Starting from the ground-

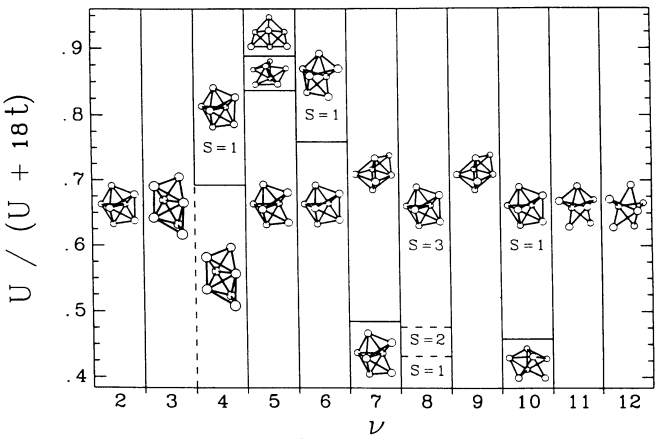

FIG. 3. Phase diagram of Hubbard clusters having $N = 7$ atomic sites and large values of U/t. As in the previous figures, the ground-state spin S is indicated only if $S \geq 1$.

state structures for $U = 0$ [8], one typically observes that as U is increased, first one or more of the weakest cluster bonds are broken. This change to more open structures occurs for $U/t \simeq 1$–4 and is most often seen for $\nu < N$, since in this case the $U = 0$ structures are more compact, while for $\nu > N$ the structures are rather open already for $U \to 0$ (see Figs. 1 and 2). As U is further increased ($U/t > 5$–6) it is energetically more advantageous to create additional new bonds. Higher coordination gives the strongly correlated electrons more possibilities for performing a mutually avoiding motion, and this tends to lower the kinetic energy. Moreover, these compact structures are more symmetric. Therefore, the electron-density distribution is more uniform, which also contributes to lower the Coulomb-repulsion energy.

It is interesting to compare our results for $\nu = N, N \pm 1$ with first principles calculations for simple-metal clusters [16]. Previous Hückel calculations [8] have already shown that the optimal structures for $U = 0$ and $\nu = N$ are in good agreement with *ab initio* results for neutral clusters ($N \leq 9$). Including the Coulomb interactions we now show that for $\nu = N$ these structures remain stable up to $U/t \simeq 4$–8, i.e., far beyond the weakly correlated limit. This explains the success of the $U = 0$ calculations in applications to these real systems, which are of course correlated, though not very strongly. For cations ($\nu = N - 1$) the situation is similar except for $N = 5$ and $N = 6$ where the results for $U > 0$ agree with the *ab initio* calculations, while the results for $U \to 0$ disagree with them. This suggests that in these cases the correlation effects play an important role in determining the relative stabilities [17]. Our results for $\nu = N + 1$ and $N \leq 6$ disagree with the *ab initio* structures reported in Ref. [16] for Li_N^-. This could be an indication of the breakdown of the single-band tight-binding approximation for states close to the continuum [10,18].

The structural changes at larger U are often accompanied by strong changes in the magnetic behavior. One may indeed say—as already pointed out by Callaway *et al.* [7]—that these structural changes are driven by magnetism. For half-band filling ($\nu = N$) the optimal structures show minimal total spin S and strong antiferromagnetic correlations. None of the structures having a (unsaturated) ferromagnetic ground state [19] (e.g., "stars") were found to be the most stable ones for any value of U/t. The optimal antiferromagnetic structures are *nonbipartite* (see Figs. 1 and 3). For instance, the rhombus is more stable than the square for $N = \nu = 4$. The bonds, which are "frustrated" in a static picture of antiferromagnetism, yield an appreciable energy lowering when quantum fluctuations are taken into account. Therefore, Hubbard clusters with one electron per site and large U/t can be best seen as frustrated quantum antiferromagnets.

For all studied cluster sizes ($N \leq 8$), the most stable structures for $\nu = N + 1$ show ferromagnetism for large U (typically $U/t > 4$–14). This is in agreement with Nagaoka's theorem [20]. For the smaller clusters, i.e., $N = 3$, 4, and 6, this is the only case where the optimal structures are ferromagnetic. For $N = 5$ unsaturated ferromagnetism ($S = 1$) is also found for $\nu = 4$, though at large values of U ($U/t > 30$). However, for larger clusters, ferromagnetism extends more and more throughout the U/t-ν/N phase diagram. Indeed, for $N = 7$ ferromagnetism is found for $\nu = 4$, 6, 8, and 10 (see Fig. 3). Clusters with $N = 8$ can be ferromagnetic for $\nu = 9$–12. The tendency towards ferromagnetism is much stronger for more than half-band filling than for $\nu \leq N$. This is qualitatively in agreement with experiments on $3d$ TM clusters. In fact one observes that the magnetic moments per atom μ in V and Cr clusters are very small if not zero [$\mu < (0.6$–$0.8)\mu_B$] [21], while Fe and Co clusters show large magnetizations [1,2,22]. Finally, let us remark that the appearance of ferromagnetism is much less frequent than what one would expect from mean-field Hartree-Fock arguments (Stoner criterion). This reveals, once more, the importance of correlations in low-dimensional systems [5–7]. However, the model of Hubbard clusters exaggerates the effects of quantum fluctuations being one of the most extremely low-dimensional systems one can consider. Improvements on the model, by including either several bands or nonlocal interactions, would tend to weaken such strong fluctuation effects.

As important as identifying the existence of ground-state ferromagnetism in small clusters ($S \geq 1$) is determining the stability of the ferromagnetic state at $T > 0$ and characterizing the microscopic mechanisms responsible for the temperature dependence of S. For this purpose we have computed the excitation energy ΔE from a ferromagnetic ground state to the lowest lying nonferromagnetic state (i.e., $S = 0$ or $1/2$). The energy $\Delta E = E(S = 0, 1/2) - E(S \geq 1)$ gives a measure of the temperature $T_c \simeq \Delta E/k_B$ at which the ferromagnetic correlations are strongly reduced by thermal excitations. Notice that the excitations ΔE can be of mainly two different kinds. One can perform a purely *electronic excitation* $\Delta E_{\rm el}$, where the cluster structure remains fixed to the optimal structure at $T = 0$. Or one can perform a purely *structural change* $\Delta E_{\rm st}$, where the electrons remain in the ground state and the structure is changed until the ground state corresponding to this new structure shows no ferromagnetism. In Fig. 4 the exact calculated $\Delta E_{\rm el}$ and $\Delta E_{\rm st}$ are shown for $\nu = N + 1$, $U/t = 64$, and $N \leq 8$. As already discussed, in these cases the optimal structures at $T = 0$ are very compact and show saturated ferromagnetism [i.e., $S = 1/2(N - 1)$]. The remarkable new result is that $\Delta E_{\rm el}$ and $\Delta E_{\rm st}$ have similar values, and that $\Delta E_{\rm st}$ can even be smaller than $\Delta E_{\rm el}$. This implies that the *structural changes* are at least as important as the *electronic excitations* for determining the temperature dependence of the magnetization of small clusters. Experimentally, there might be indications that for Fe_N structural changes could be related to the drop of the magnetization observed for increasing T [22]. From the points of view of theory, it still remains to be proven

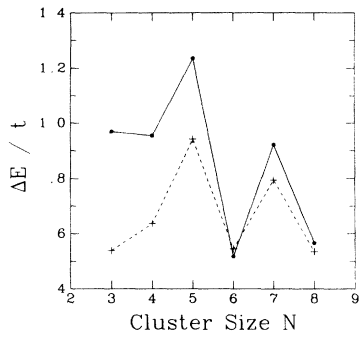

FIG. 4. Size dependence of the spin excitation energy ΔE from the ferromagnetic ground state ($S \geq 1$) having the optimal cluster structure to the lowest lying nonferromagnetic state ($S = 0$ or $S = 1/2$). The full line corresponds to a purely *electronic excitation* and the broken line to a purely *structural change*. The number of electrons is $\nu = N + 1$ and the Coulomb-repulsion strength is $U/t = 64$.

whether the conclusions obtained from the calculation of ΔE_{el} and ΔE_{st} within the Hubbard model are also valid for more realistic models (e.g., including the d-band degeneracy and/or interatomic Coulomb interactions). If this would be so, the mechanisms responsible for the temperature dependence of the magnetization of small $3d$ TM clusters could be intrinsically different from those known in the solid state.

The properties of small clusters ($N \leq 8$) were studied here in the framework of the Hubbard model, and for the first time a solution of the many-body problem was achieved which is *complete* from both the electronic and the structural points of view. Extensions of this work by improving the Hamiltonian are certainly desirable and necessary for a more realistic description of magnetic materials. Nevertheless, the rigorous results presented here should always preserve their relevance due to the fundamental and universal character of the model, and as a reference for future studies.

This work has been supported by the Deutsche Forschungsgemeinschaft through SFB 341.

[1] W.A. de Heer, P. Milani, and A. Châtelain, Phys. Rev. Lett. **65** 488 (1990).

[2] J.P. Bucher, D.G. Douglas, and L.A. Bloomfield, Phys. Rev. Lett. **66**, 3052 (1991).

[3] K. Lee, J. Callaway, and S. Dhar, Phys. Rev. B **30**, 1724 (1985); K. Lee, J. Callaway, K. Wong, R. Tang, and A. Ziegler, *ibid.* **31**, 1796 (1985); K. Lee and J. Callaway, *ibid.* **48**, 15 358 (1993).

[4] G.M. Pastor, J. Dorantes-Dávila, and K.H. Bennemann, Physica (Amsterdam) **149B**, 22 (1988); Phys. Rev. B **40**, 7642 (1989).

[5] L.M. Falicov and R.H. Victora, Phys. Rev. B **30**, 1695 (1984).

[6] Y. Ishii and S. Sugano, J. Phys. Soc. Jpn. **53**, 3895 (1984).

[7] J. Callaway, D.P. Chen, and R. Tang, Z. Phys D **3**, 91 (1986); Phys. Rev. B **35**, 3705 (1987).

[8] Y. Wang, T.F. George, D.M. Lindsay, and A.C. Beri, J. Chem. Phys. **86**, 3493 (1987).

[9] J. Hubbard, Proc. R. Soc. London A **276**, 238 (1963); *ibid.* **281**, 401 (1964); J. Kanamori, Prog. Theor. Phys. **30**, 275 (1963); M.C. Gutzwiller, Phys. Rev. Lett. **10**, 159 (1963).

[10] Further details will be published elsewhere.

[11] For $N \geq 7$ some physical considerations should be made. Here we find graphs (e.g., the pentagonal bipyramid) which do not satisfy the previous conditions but which are *physically* acceptable as structures since the conditions are only slightly violated. Therefore, we have also considered these graphs as possible cluster structures. The magnetic properties of the Hubbard model on arbitrary graphs will be discussed elsewhere.

[12] Taking into account all possible structures involves a large computational effort. For instance, for $N = 7$ and $N = 8$ there are, respectively, 853 and 11 117 nonequivalent graphs. In fact, it is the exploding number of possible geometrical configurations that limits our present study to $N \leq 8$.

[13] C. Lanczos, J. Res. Nat. Bur. Stand. **45**, 255 (1950); B.N. Parlett, *The Symmetric Eigenvalue Problem* (Prentice-Hall, Engelwood Cliffs, 1980).

[14] Throughout this work the term "exact" should be understood as exact within the accuracy $\varepsilon \simeq 10^{-10}$ when it refers to energies.

[15] Physically, varying U/t can be viewed as changing the interatomic distance (e.g., $t \propto R_{ij}^{-5}$) or changing the spatial extension of the valence wave function (i.e., the element). Different ν/N can be related either to simple metal clusters in different ionic states ($\nu = N, N \pm 1$) or, more indirectly, to different elements in a TM series. These analogies provide our study with a more universal character.

[16] V. Bonačić-Koutecký, P. Fantucci, and J. Koutecký, Chem. Rev. **91**, 1035 (1991), and references therein.

[17] We do not obtain the optimal structures reported in [16] for Li_4^+ and Li_5^+. The optimal Hubbard structure corresponds in these cases to the second-best *ab initio* structure. Notice, however, that often the energy differences are small and in some cases different *ab initio* approximations yield somewhat different geometries (Ref. [16]).

[18] The Hubbard model is in accordance with nature in a further interesting aspect. While the number of possible lattice configurations or graphs n_g increases in a very explosive way with the number of atoms N, the number of structures n_o which are optimal for some value of the parameters U/t and ν/N remains a handful. For example, for $N = 7$ (8), $n_g = 853$ (11117) while $n_o = 18$ (23). As the cluster size increases, some growth patterns start to dominate and the same or very similar structures cover large regions of the phase or structural diagram (see Figs. 2 and 3). The situation tends to what one observes in the macroscopic limit (solid state) as we go through the periodic table of the elements (see Ref. [15]).

[19] E.H. Lieb, Phys. Rev. Lett. **62**, 1201 (1989).

[20] Y. Nagaoka, Phys. Rev. **147**, 392 (1966); H. Tasaki, Phys. Rev. B **40**, 9192 (1989).

[21] D.C. Douglass, J.P. Bucher, and L.A. Bloomfield, Phys. Rev. B **45**, 6341 (1992).

[22] I.M.L. Billas, J.A. Becker, A. Châtelain, and W.A. de Heer, Phys. Rev. Lett. **71**, 4067 (1993).